Eur. Phys. J. D **28**, 393–398 (2004)
DOI: 10.1140/epjd/e2003-00324-1

THE EUROPEAN PHYSICAL JOURNAL D

Intensity dependence of hydrogen Lyman alpha and Balmer alpha lines upon cathode material of an abnormal glow discharge

M. Gemišić Adamov[1], M.M. Kuraica[1,2], and N. Konjević[2,a]

[1] Center for Science and Development of Technology, Obilicev Venac 26, 11001 Belgrade, Serbia and Montenegro
[2] Faculty of Physics, University of Belgrade, P.O. Box 368, 11001 Belgrade, Serbia and Montenegro

Received 23 May 2003 / Received in final form 17 November 2003
Published online 20 January 2004 –

Abstract. The results of the hydrogen L_α 121.567 nm and H_α 656.280 nm line intensity dependence upon cathode material of an abnormal glow discharge are reported. Under similar experimental conditions systematic variation of the L_α and H_α line intensity with the atomic number Z of cathode material (graphite, Ti, Fe, Cu, Zn, Pd, Ag, Pt, Au and Pb) is detected. Shapes of line intensity Z-dependences suggest that, apart from electron impacts, line excitation is related also to the back-scattering of fast hydrogen atoms from cathode and sputtering yield of cathode material. The excitation of H_2 molecular bands is not sensitive to these cathode processes.

PACS. 32.30.Jc Visible and ultraviolet spectra – 32.70.-n Intensities and shapes of atomic spectral lines – 52.80.Hc Glow; corona – 52.70.Kz Optical (ultraviolet, visible, infrared) measurements – 52.20.Hv Atomic, molecular, ion, and heavy-particle collisions – 52.40.Hf Plasma-material interactions; boundary layer effects

1 Introduction

It is well-known that the largest amount of radiation from a glow discharge comes from the negative glow region [1]. Here, we excluded from consideration plasma column, which is not present in studied abnormal glow discharge. Main processes responsible for emission of radiation in the negative glow region involve electron interaction with molecular, atomic and ionic species. In the case of hydrogen glow discharge however, strong Balmer lines emission comes from the cathode fall region [2]. The explanation of "unusual" hydrogen line emission is related to hydrogen atomic and molecular ions H^+, H_2^+ and H_3^+ present under typical discharge conditions. In the cathode fall region accelerated ions exchange electric charge with hydrogen molecules and, as a result, fast neutrals and slow ions appear see e.g. [2–4]:

$$(H^+)_f + (H_2)_s \rightarrow H_f^* + (H_2^+)_s, \quad (1)$$

$$(H_2^+)_f + (H_2)_s \rightarrow H_f^* + H_f + (H_2^+)_s, \quad (2)$$

$$(H_3^+)_f + (H_2)_s \rightarrow H_f^* + (H_2)_f + (H_2^+)_s, \quad (3)$$

where with f and s fast and slow particles are denoted respectively.

It is shown [5–9] that particles (H^+, H_2^+, H_3^+, H_2 and H) having energies of the order of magnitude of 10^2 eV are back-scattered from cathode in the form of fast hydrogen atoms, H. The number and the energy of back-scattered atoms depends upon cathode material while their spatial distribution is proportional to $\cos^2\Theta$ where Θ is the angle in respect to the axis perpendicular to the cathode surface [7–9].

The main sources of fast exited hydrogen atoms are H^+ and H_3^+ ions (exhibit an asymmetrical charge-exchange reaction in collisions with H_2), which are, as a consequence of relatively low cross-sections for collisions, efficiently accelerated towards cathode, see e.g. [2–4]. Some of these ions on their way to the cathode collide with the matrix gas, H_2, and with sputtered cathode material producing fast exited neutrals, H^*. The rest of accelerated ions reach cathode where they neutralize, or neutralize and fragmentize. The back-reflected particles from cathode are fast H atoms directed back to discharge. After collisions of these fast H atoms with H_2 and/or with other discharge constituents, fast excited atoms, H^*, are produced as well. These fast excited hydrogen atoms moving towards and from the cathode are detected in different discharges in pure hydrogen and in hydrogen mixtures with inert gases [2–4,10–22] by means of Doppler spectroscopy of Balmer lines. Depending upon discharge conditions, excited hydrogen atoms with energies ranging from several tens up to several hundreds eV are detected. Recently, Mills et al. [23] reported excessive H_α broadening corresponding to excited atom temperatures of 23–45 eV in a glow discharge with Sr–H_2, Sr–Ar–H_2, Sr–He–H_2 and He–H_2 mixtures.

[a] e-mail: nikruz@ff.bg.ac.yu

The influence of cathode material on the hydrogen line shapes is reported for the first time by Li Ayres and Benesh [11]. When Cu cathode in glow discharge is replaced with Ni, no change in the line shape is detected [11]. However, if parts of the cathode along the observation direction are covered with rubber, the shape of hydrogen lines changed considerably [11]. For the H_α line shape recordings Petrovic et al. [3] used cathode made of thin transparent layer of Au and Pt (observations of line shapes are performed through this electrode) and graphite anode. The comparison of this line shape with the one recorded with graphite cathode [3] showed large difference, indicating that relationship between cathode material and energy of fast excited hydrogen atoms exists.

First systematic study of the influence of cathode material to the shape of hydrogen H_α line in an abnormal glow discharge is reported by Kuraica and Konjević [19]. They studied H_α line shapes with Fe, Cu, Zn, Ag, Sn, Au, Pb and Bi cathodes in pure hydrogen and in $Ne + 3\%H_2$ mixture. Although the contribution of extended line wings to the whole line profile depends to a large extent upon matrix gas, the same characteristic overall dependence upon atomic number Z of the cathode material is detected for both gases, H_2 and $Ne+3\%H_2$, [19]. The authors in [19] related these Z dependences with maxima for Cu, Ag and Au, to the amount of sputtered cathode material in discharge, which increases the total cross-section for fast hydrogen atom excitation.

In this paper we extend study intensity dependence of visible hydrogen lines upon cathode material in an abnormal glow discharge to the VUV L_α line. The study of the L_α and referent H_α line is performed with larger number of cathode materials than previously reported for the H_α line [19]. On the basis of these results an explanation of line intensity vs. atomic number Z dependence is offered with new details not discussed before.

2 Experimental

Our discharge source, a modified Grimm glow discharge [24,25] is similar in design to that used by Fereira et al. [26], see Figure 1 in [27].

The hollow anode 30 mm long with inner and outside diameters 8.00 and 13 mm is made of brass. The water cooled cathode holder has an exchangeable electrode made of graphite (99.9998%), Ti (99.5%), Fe (99.0%), Cu (99.998%), Zn (99.95%), Pd (99.99%), Ag (99.9%), Pt (99.99%), Au (99.95%) and Pb (99.7%), 5 mm long and 7.60 mm in diameter, which screws tightly onto its holder to ensure good cooling.

A gas flow of about 300 cm^3/min of hydrogen (purity 99.995%) was sustained at a selected pressure ranging between 170 and 330 Pa by means of a needle valve and a two-stage mechanical vacuum pump. In order to prevent back streaming of oil vapours, a zeolite trap is mounted between discharge vessel and vacuum pump. To run the discharge a 0–2 kV and 0–100 mA current stabilized power supply is used.

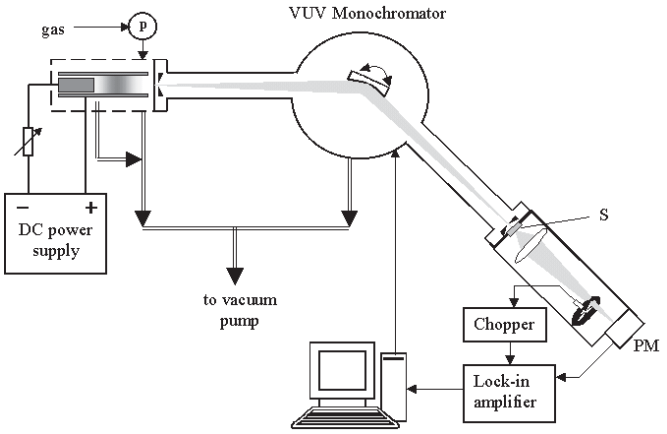

Fig. 1. Schematic diagram of the experimental setup for VUV spectra recordings; P-pressure gauge, S-scintillator and PM is photomultiplier.

The schematic diagram of the experimental set-up for the L_α study is given in Figure 1. The cathode-anode position is set for end-on discharge observations. The discharge is mounted directly on the entrance slit of the Seya-Namioka type monochromator equipped with toroidal diffraction grating (horizontal and vertical radius 1000 mm and 103 mm respectively) with 275 grooves/mm (reciprocal dispersion 2 nm/mm). With the width of entrance and exit slit of 0.1 mm the instrumental halfwidth is 0.3 nm. Prior to the experiment, the monochromator and the discharge chamber are evacuated with the same mechanical vacuum pump, see Figure 1 to the pressure of 10 Pa.

Behind the exit slit of the monochromator a glass window is mounted with a coating of sodium salicilate (used to convert VUV into visible blue) facing the incident radiation. The light chopper is used in conjunction with a lock-in-amplifier to detect radiation focussed with a lens (focal length 60 mm) onto the photomultiplier's cathode.

For the H_α end-on observations the discharge image, 1:1 magnification, is projected with lens (150 mm focal length) onto an optical fiber that transfers radiation to the entrance slit of 1 m Chzerny-Turner monochromator equipped with 1200 g/mm diffraction grating (0.811 nm/mm inverse linear dispersion in the first diffraction order) blazed at 600 nm. At the place of the exit slit CCD multichannel detector (2048 pixels each 14 μm wide) is used. With the entrance slit of 35 μm the instrumental profile halfwidth was 0.036 nm. The instrumental profile is determined by recording same lines from a low pressure hollow cathode discharge lamp.

3 Experimental results and discussion

Small Doppler broadening of emitted lines and low spectral resolution of our VUV monochromator prevented the L_α line shape studies and therefore line intensities are observed only. An example of spectra recordings in the range

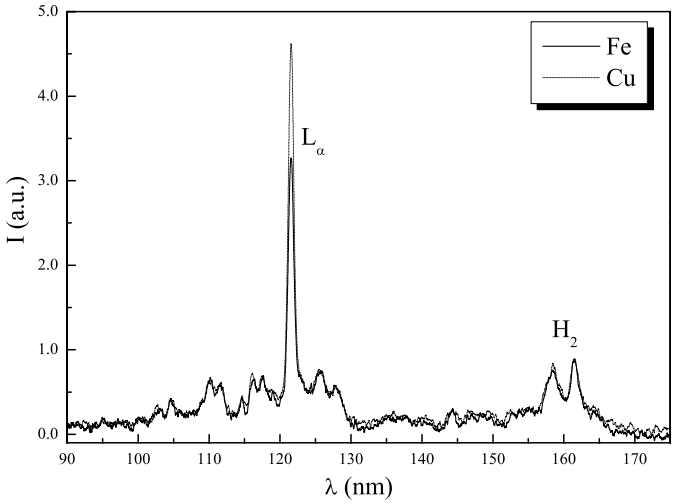

Fig. 2. VUV hydrogen spectra with Cu and Fe cathode. Hydrogen pressure 330 Pa, power input 15 W.

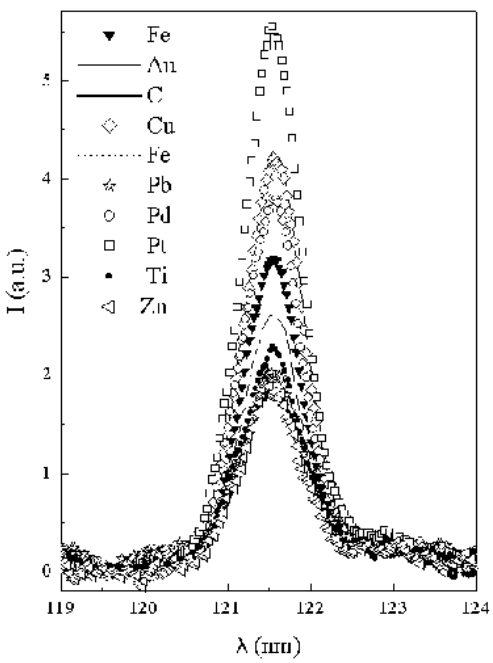

Fig. 3. Recordings of the L_α line with different cathodes. Hydrogen pressure 330 Pa, power input 15 W.

90 nm through 175 nm with Fe and Cu cathode under similar experimental conditions are shown in Figure 2. The intensity of molecular hydrogen spectra, in particular region around 160 nm, are identical with both cathodes indicating same level of excitation. Under similar discharge conditions intensities of the L_α line with Cu and Fe cathode differ, indicating in this way that the line excitation mechanism is partially different from the one responsible for molecular bands.

In order to study the L_α line intensity dependence upon atomic number Z of cathode material, in addition to Fe and Cu cathodes, eight other cathodes are used under similar experimental conditions and examples of line recording are given in Figure 3. In these spectra the hydrogen molecular bands do not show any variation compared to spectra in Figure 2. The dependence of L_α line intensity upon Z of cathode material is given in Figure 4. Solid and dashed lines drawn between experimental data in this figure have no physical meaning and they are used to facilitate comparison only.

The comparison of results in Figure 4 indicates that, apart from always present electron excitation, other excitation mechanisms of the L_α line exist. The origin of these excitation processes may be related to reactions (1–3). The accelerated hydrogen ions and atoms on their way to cathode collide with matrix gas, H_2, and sputtered cathode material, while fast back-scattered hydrogen atoms also collide with the same discharge constituents. Since in all experiments same matrix gas is used, the difference of L_α line intensities may result from the difference in sputtering yields of cathode materials and cross-sections for the L_α line excitation in collisions of fast H atoms and hydrogen ions with sputtered particles. Furthermore, since the flux and energy of back-scattered fast H atoms from the cathode depend upon cathode material, in addition to collision processes in discharge, reflection coefficients of cathode should be taken into consideration also. Since all relevant processes for the L_α line excitation are of importance for H_α line as well, they will be discussed after presenting results for this line.

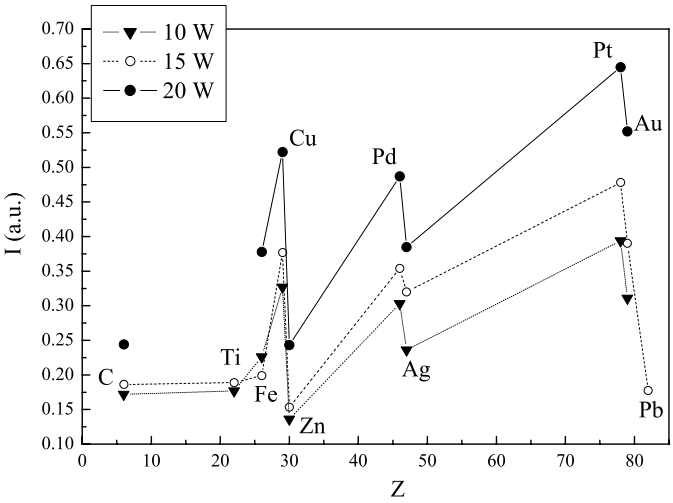

Fig. 4. Intensity of the L_α line recorded with different cathodes. Hydrogen pressure 330 Pa.

Typical H_α line profile is given in Figure 5. The peculiar line shape is detected and discussed in a number of experiments, see e.g. [4,10–13,15,16,18–20] and will not be discussed here in details. We shall point out only that narrow central part of profile is emitted from the negative glow region while widely broadened wings are emitted from the whole discharge starting from the cathode surface, see e.g. [2] and Introduction. Similar shape is expected for the L_α line but, due to low resolution of our VUV monochromator, it is not possible to prove experimentally this expectation. Since intensities of the L_α line are measured only, integral intensities of the H_α line are

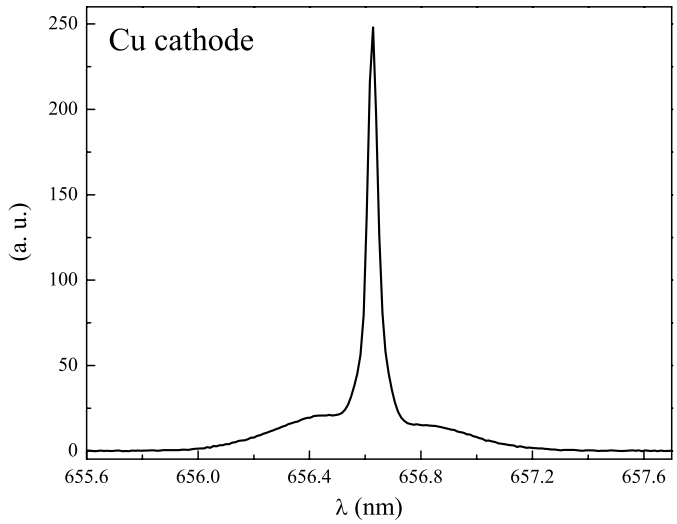

Fig. 5. Typical H_α line shape. Experimental conditions: voltage 1000 V, current 15.5 mA and hydrogen pressure: 330 Pa.

Table 1. Normal incidence cathode surface reflectivity R at the H_α and L_α wavelengths. Estimated uncertainties for the measured H_α reflectivities: 10% and 20% for $R > 0.5$ and $R < 0.5$ respectively.

Element	Reflectivity at the H_α		Reflectivity at the L_α
	measured	from [28]	from [28]
C	0.14		
Ti	0.37	0.54	0.18
Fe	0.38	0.56	0.20
Cu	0.70	0.94	0.13
Zn	0.51		
Pd	0.51	0.73	0.09
Ag	0.84	0.94	0.08
Pt	0.53	0.68	0.21
Au	0.81	0.97	0.13
Pb	0.06		

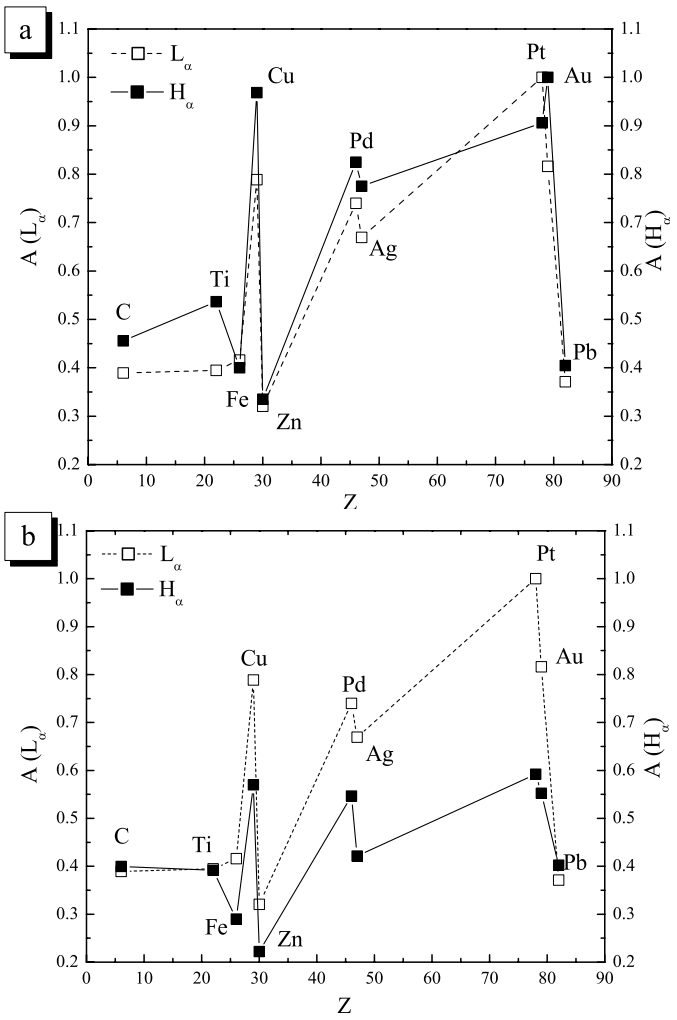

Fig. 6. Comparison of L_α and H_α intensities versus atomic number Z of cathode material: (a) without correction for cathode surface reflection and (b) corrected for the cathode reflection at H_α wavelength.

used for comparison and results are given in Figure 6a. As expected, the Z-dependences are similar for both lines what is also an indication that self-absorption of the L_α line did not influence to the larger extent line intensity measurements. It is important to note that the L_α and H_α profiles in Figures 2–6a are recorded from the discharge observed end-on, see Figure 1, and therefore the reflected radiation from the cathode surface contributed to the total line intensity. Since the reflectivity at the H_α wavelength varies from one cathode material to another, the measurement of cathode surface reflectivity is always performed after line recording and results are given in Table 1. Since the normal incidence reflectivity at the L_α wavelength is small, see [28] and Table 1, the reflectivity measurements at this wavelength are not performed. This is further justified by the fact that measured reflectivity at the H_α wavelength are always smaller than data in [28], see results in Table 1.

The corrected H_α line intensity Z-curve is given together with the corresponding curve for the L_α line in Figure 6b. As expected both curves show similar Z-behaviour.

The increase of the L_α intensities in Figure 4 for larger electrical power inputs induced mainly by an increase of voltage is expected also. Namely, for higher voltages, ion and electron energy raise and excitation rate increases. Similar results are obtained for the H_α line wings, which are studied separately from the rest of line profile [29]. As already pointed out earlier, an attempt will be made to assess the importance of two cathode processes indirectly responsible for hydrogen lines excitation: back-scattering of fast hydrogen atoms and sputtering induced by H^+ ions.

First, back-scattering coefficients of H^+ ions, which are reflected from cathode as fast H atoms, are taken from [30], for the ion energies of few hundred eV expected in our discharge. To our knowledge corresponding data for hydrogen molecular ions are not available. Two reflection coefficients are considered here: one is the number scattering coefficient R_N, representing the ratio of scattered

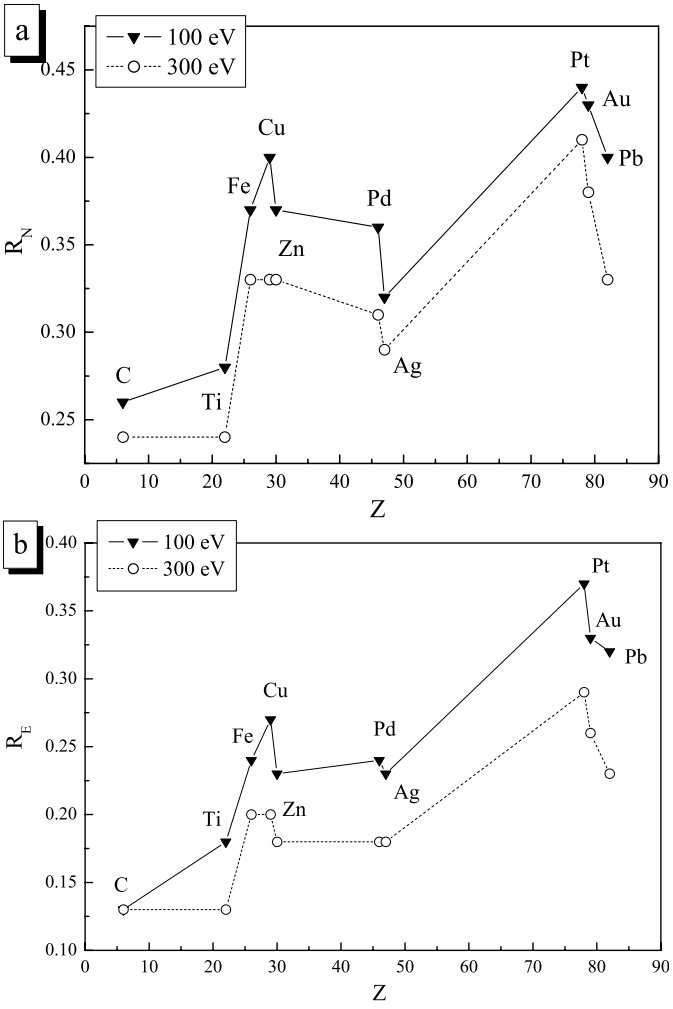

Fig. 7. Z-dependence of back scattering coefficients for normal incidence H^+ ions, data taken from [30]: (a) number reflection coefficient R_N and (b) energy reflection coefficient R_E.

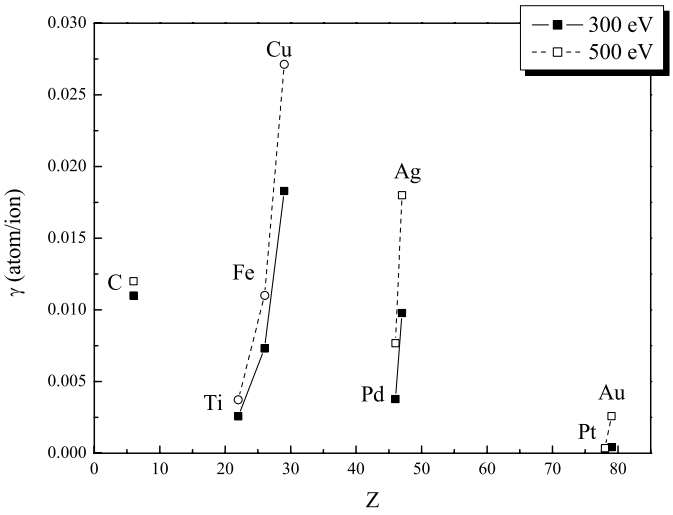

Fig. 8. Sputtering yields for normal incidence H^+ ions calculated from semiempirical formula [31].

particles number to the incoming ones and second is the energy scattering coefficient, R_E, that represents ratio of total scattered particles' energy to the energy of incoming particle. These coefficients are used successfully with Pd–Au electrode to explain the emission characteristics of a low current, DC discharge in hydrogen [3]. In our case coefficients R_N and R_E are employed only to compare shapes of $R_N(Z)$ and $R_E(Z)$, see Figures 7a and 7b with those in Figures 4 and 6b. With higher reflection coefficients one has larger flux of fast H atoms with higher energies, coming from the cathode. Larger flux of fast H atoms is responsible for an increase of total line intensity. With larger energies they are more efficiently excited in collisions with hydrogen molecules enlarging in this way total line intensity.

It is important to notice that both coefficients R_N and R_E decrease with an increase of H^+ incident energy. On the other hand H^+ sputtering yield increases with incident energy, see Figure 8. Data in this figure are calculated from the following semiempirical formula [31]:

$$Y(E) = 0.042 \frac{Q(Z_2)\alpha(M_2/M_1)}{U_s} \frac{S_n(E)}{1 + \Gamma k_e \varepsilon^{0.3}} \left[1 - \sqrt{\frac{E_{th}}{E}}\right]$$

where the Γ factor has the following expression: $\Gamma = W(Z_2)/[1 + (M_1/7)^3]$, $W(Z_2)$, $Q(Z_2)$ and s are listed in Table 1 [31], α is the function of mass ratio [31], $S_n(E)$ is the nuclear stopping cross-section, E_{th} is the sputtering threshold energy, k_e is the Lindhard stopping coefficient, U_s is the surface binding energy, ε is the reduced energy, Z_1 and Z_2 are the atomic numbers, and M_1 and M_2 the masses of the projectile and the target atom respectively. Here, the sputtering induced by ions of ejected cathode material is not taken into account. All necessary data for the sputtering yield evaluations are taken from [31].

It is interesting to compare the Z-dependence of measured L_α and H_α line intensities in Figures 4 and 6b with data in Figures 7 and 8. With exception of Cu maximum, the Z-dependence of back-scattering coefficients R_N and R_E have maximum for Pd and Pt, see Figures 7a and 7b while sputtering yield is largest for Ag and Au, see Figure 8. Maxima of measured L_α and H_α line intensities are for Pd and Pt in Figures 4 and 6b illustrate the importance of back-scattered fast H atoms from cathode for hydrogen lines excitation. In the case of Cu, both, back-scattering and sputtering have maxima and therefore both lines are very strong, see Figures 4 and 6b.

4 Conclusion

The experimental study of the VUV and visible spectra of hydrogen glow discharge with different cathode materials shows that partly different excitation mechanisms govern excitation of the L_α and H_α lines in respect to those responsible for excitation of hydrogen molecular bands. Similar shapes of the L_α and H_α line intensity Z-dependence

curves, see Figures 4 and 6, and shapes for H^+ number, R_N, and energy, R_E, reflection coefficients and sputtering yield maximums, see Figures 7 and 8, indicate that both, reflection of fast H atoms and sputtering of cathode material, are of importance for excitation of hydrogen lines. The excitation of H_2 molecular bands however, is not sensitive to these two cathode processes. The shapes of Z-dependences for L_α and H_α intensities in Figure 6b suggest similar excitation mechanisms for both lines.

This work within the Project 1736 is partially supported by the Ministry of Science, Technology and Development of the Republic of Serbia. The authors gratefully acknowledge discussions with B.M. Obradović.

References

1. A. von Engel, *Ionized gases* (Clarendon Press, Oxford, 1965)
2. I.R. Videnović, N. Konjević, M.M. Kuraica, Spectrochim. Acta B **51**, 1707 (1996)
3. Z.Lj. Petrović, B.M. Jelenković, A.V. Phelps, Phys. Rev. Lett. **68**, 325 (1992); Z.Lj. Petrović, in *Joint Symposium on Electron and Ion Swarms and Low Electron Scattering* (Bond University, Gold Coast, Queensland, 1991), p. 58
4. N. Konjević, I.R. Videnović, M.M. Kuraica, J. Phys. France **7**, C4-247 (1997)
5. G.M. McCracken, Rep. Prog. Phys. **38**, 241 (1975)
6. T. Gotoh, M. Kotani, Y. Kawaguchi, Y. Tazawa, Y. Shigeta, S. Ohtani, J. Phys. D **16**, 439 (1983)
7. W. Eckstein, J.P. Biersuck, Appl. Phys. A **38**, 123 (1985)
8. R. Aratari, W. Eckstein, J. Nucl. Mat. **162-164**, 910 (1989)
9. R. Aratari, W. Eckstein, Nucl. Instrum. Meth. Phys. Res. B **42**, 11 (1989)
10. W. Benesh, E. Li, Opt. Lett. **9**, 338 (1984)
11. E.Li Ayers, W. Benesh, Phys. Rev. A **37**, 194 (1988)
12. A.L. Cappelli, R.A. Gottscho, T.A. Miller, Plasma Chem. Plasma Proc. **5**, 317 (1985)
13. G. Sultan, G. Baravian, M. Gantois, G. Henrion, H. Michel, A Ricard, Chem. Phys. **123**, 423 (1988)
14. A.M. Bruneteau, G. Hollos, M. Bacal, J. Appl. Phys. **67**, 7254 (1990)
15. C. Barbeau, J. Jolly, J. Phys. D **23**, 1168 (1990)
16. M. Kuraica, N. Konjević, Phys. Rev. A **46**, 4479 (1992)
17. S. Djurovic, J.R. Roberts, J. Appl. Phys. **74**, 6558 (1993)
18. B.P. Lavrov, A.S. Mel'nikov, Opt. Spectrosc. **75**, 1152 (1993)
19. M. Kuraica, N. Konjević, Phys. Scripta **50**, 487 (1994)
20. B.P. Lavrov, A.S. Mel'nikov, Opt. Spectrosc. **79**, 922 (1995)
21. S. Radovanov, J.K. Olthoff, R.J. van Brunt, S. Djurovic, J. Appl. Phys. **78**, 746 (1995)
22. S.B. Radovanov, K. Dzierzega, J.R. Roberts, J.K. Olthoff, Appl. Phys. Lett. **66**, 2637 (1995)
23. R.L. Mills, M. Nansteel, P.C. Ray, IEEE Trans. Plasma Sci. **30**, 639 (2002)
24. W. Grimm, Naturwiss. **54**, 586 (1967)
25. W. Grimm, Spectrochim. Acta B **23**, 443 (1968)
26. N.P. Ferreira, H.G.C. Human, L.R.P. Butler, Spectrochim. Acta B **35**, 287 (1980)
27. M. Kuraica, N. Konjević, M. Platiša, D. Pantelić, Spectrochim. Acta B **47**, 1173 (1992)
28. *CRC Handbook of Chemistry and Physics*, edited by R.C. Weast, 64th edn. (CRC Press Inc., Boca Raton, Florida, 1984)
29. M. Gemišić-Adamov, B. Obradović, M.M. Kuraica, N. Konjević, IEEE Trans. Plasma Sci. **31**, 444 (2003)
30. T. Tabata, R. Ito, Y. Itikawa, N. Itoh, K. Morita, At. Data Nucl. Data Tables **28**, 493 (1983)
31. Y. Yamamura, H. Tawara, NIFS-data **23**, Mar. 1995